Progress Report on Long-Term Thermal Performance of Polyisocyanurate Boardstock Materials

Bomberg, M. T.; Kumaran, M. K.

Publisher's version / Version de l'éditeur:
https://doi.org/10.4224/20375612
Internal Report (National Research Council of Canada. Institute for Research in Construction), 1991-01

National Research Council Canada | Conseil national de recherches Canada

Institute for Research in Construction | Institut de recherche en construction

Progress Report on Long-Term Thermal Performance of Polyisocyanurate Boardstock Materials

M.T. Bomberg and M.K. Kumaran

Internal Report No. 603

Date of Issue: January 1991

This internal report, while not intended for general distribution, may be cited or referenced in other publications.

Canada

Progress report on long-term thermal performance of polyisocyanurate boardstock materials

by

M.T. Bomberg and M.K. Kumaran

ABSTRACT

Following a successful application of slicing and scaling techniques to predict the long-term performance of sprayed polyurethane foams, three types of generic boardstock products were examined in this work. The conclusion is that the scaling approach may not be directly applicable to faced or non-uniform boardstock products.

The results shown in this report indicate, however, that preparing specimens with a partial encapsulation technique developed during this research and measuring aging curves on these specimens may help in the quality assurance of the boardstock products.

INTRODUCTION

In 1989 the Society of Plastics Industry (SPI) and the National Research Council (NRC) initiated a joint research program with a mission : "To initiate and undertake Canadian research and development activity in cellular plastic technologies to improve their field performance". One of the objectives of this program is to develop a methodology for predicting long-term thermal performance of foams manufactured with alternative blowing agents.

One of such predictive techniques, using time dependence of thermal resistivity (aging curves) established on thin material layers to predict thermal performance for the full product thickness by means of scaling, was previously applied to spray polyurethane foams. As described in previous publications (Bomberg & Kumaran [1], Kumaran & Bomberg [2]), this technique involves three stages:

1) selecting and preparing thin specimens that would adequately represent the product (slicing),

2) evaluating differences between slices selected from different locations and to establish the dependence of thermal resistivity on aging time, (characteristic aging curve of the product) and

3) predicting aging of the full thickness board (scaling)

The following report presents research performed at the Institute for Research in Construction (NRC-IRC) assessing the applicability of the scaling technique to three types of generic polyisocyanurate boardstock products.

MATERIAL SELECTION

Two unfaced and one faced polyisocyanurate (PIR) products were manufactured with CFC 11:

> PIR product A was an unfaced product; formulation and moulding conditions were selected to produce skins,
>
> PIR product B was manufactured as a steel faced panel but tested with the facing material removed,
>
> PIR product C was a free-rise foam faced with gas barriers and produced on a commercial equipment as 25 mm thick, 1.2 m x 2.4 m boards.

Product A was designed and manufactured in a small and well controlled moulding press with a view to achieving large differences in density of the surface and core layers. In effect, one surface layer had a density of approximately 62 kg/m^3, the other 52 kg/m^3, while the middle layers were close to 32 kg/m^3, see Figure 1. Thickness of the board was approximately 73 mm.

The panel from which product B was retrieved had a nominal thickness of 75 mm and was manufactured under a pilot, commercial operation. The outer layers were excluded from the testing since extensive surface damage was observed after removal of the metal facings. Density showed only slight variation (27 kg/m^3 in the middle core and 32 kg/m^3 in the layers close to the surface).

Product C, manufactured at nominal density of 27-28 kg/m^3, showed a high degree of uniformity across the cross-section even though some variations in density were seen on samples cut from different boards (Table 1).

SPECIMEN PREPARATION

Different techniques for preparation of thin layers were previously discussed by Edgecombe [3]. One of them, namely cutting with a horizontal band saw was applied to all PIR specimens; then, the thickness of the destroyed surface layer (TDSL) was measured with the air displacement method, see Schwartz et al [4].

The values of TDSL were consistent for all PIR specimens prepared with the band saw. For product A, the TDSL was determined at 0.71 mm, for product B at 0.73 mm and for product C at 0.75 mm. For product C, an additional specimen preparation technique was tried, namely the surface grinding with a Carborundum disc. In the latter case, when specimens were prepared with a Carborundum grinder, the TDSL was determined at 0.50 mm, indicating lesser damage to the surface layers. Nevertheless, because of the consistency in the TDSL results, and the comparative character of this work all test specimens were prepared with a band saw.

The next stage in testing comprises determination of the aging curves of thin material layers. If the resistance to gas diffusion is similar at each of the specimen surfaces, e.g. the core specimens, then the aging curve is determined on specimens having both surfaces exposed to ambient air. If, however, a densified material layer (skin) or a gas barrier (facing) is present and expected to reduce the rate of diffusion through one specimen surface, only the diffusion through this surface is to be tested.

To eliminate gas flow through the other surface, the latter was encapsulated with an epoxy resin applied in the manner previously described by Kumaran et al [5]. Such a partial encapsulation for material with densified boundary layer (skin) is shown in Figure 2a.

Another case examined in this research, namely when the material has been provided impermeable gas barriers is also shown in this Figure. In this case, as shown in Figure 2b, after encapsulating all the surfaces except for the facer, a slot, 1 to 2 mm wide, was cut on all side surfaces, directly under the gas barrier.

The purpose of cutting the slot in a specimen provided with a gas barrier is as follows. If there was no lateral diffusion (parallel to the surface of the facer), the distance between the centre metering area (150 mm x 150 mm) and the slot cut around a 300 mm x 300 mm specimen is too large to affect thermal resistance of the specimen over a few month test period. If, however, the rate of lateral gas diffusion from the layer adjacent to the facer is much higher than that of the core material, a reduction in the specimen thermal resistance will be seen much faster.

Finally, to compare with aging rates obtained on thin core and surface layers with those obtained on full thickness board, a few full thickness (control) specimens were also tested.

RESULTS OF MEASUREMENTS

Polyisocyanurate product A

Each of two samples of this product were divided into eleven layers. To examine the rate of one-sided aging, both outer layers (number 1 and 11, with respective densities 61 and 55 kg/m^3) were subjected to type (a) encapsulation. Two core layers (number 4 and 9, with respective densities 34 and 38 kg/m^3) were tested without encapsulation.

Measurements of thermal resistivity changes during the period of laboratory aging were performed on HFM equipment described by Bomberg and Solvason [6], in accordance to slicing and scaling methodology proposed for development of an ASTM standard recommended procedure, see Kumaran and Bomberg [2]. The results of thermal resistivity measurements, recalculated to a reference thickness of 10 mm are shown in Figure 3. This Figure shows aging curves of four specimens: two, partly encapsulated surface layers (skin) and two cut from the middle part of the board (core). For each of these specimens, density, in kg/m^3, is indicated in paranthesis, see Figure 3.

Polyisocyanurate product B

After removing outer layers, four thin layers were cut out of the sample of this product and all of them were tested without encapsulation. The results of aging measurements, recalculated to the reference thickness of 10 mm are shown in Figure 4.

In addition to aging curves, one test of thermal resistivity as a function of temperature was also performed on these specimens and the results are shown in Figure 5.

Polyisocyanurate product C

Two test series were performed on the product C. Series 1 was meant for the determination of aging characteristics of thin slices from various layers and series 2 included comparison between two sizes of test specimens.
Table 1 lists all the specimens tested in the two series and summarizes all data on polyisocyanurate product C. It also lists results of the initial r-value test and conditions of testing for all specimens, and refers to Figures showing the measured aging curves. The aging curves of core specimens cut from product C are shown in Figures 6, 7 and 12 while Figures 8-11, 13 and 14 analyze the effect of gas barrier (facing layer).

ANALYSIS OF THE TEST RESULTS

Polyisocyanurate product A

Figure 3 shows thermal resistivity of skin and core layers cut from PIR product A; as stated earlier results are recalculated to the reference thickness of 10 mm. The core specimens show a typical pattern of material aging. Using the scaling technique, thermal resistivity of 45 m.K/W (6.5 per inch) shown in this Figure for one year old core layer, would correspond to 25 year of aging if the material had been 50 mm thick, see Bomberg [7]).

Thermal resistivity of the densified material of the surface layers is much lower than that of the core layers. Since the surface layers were expected to have thermal performance better than the core layers, the changes in their thermal resistivity were determined under one-sided aging experiment (partial encapsulation type (a), i.e. gas flows only though the original specimen surface). Thermal resistivity at one year aging of the reference layer is approximately 36 m.K/W (5.2 per inch).

As shown in Figure 3, thermal resistivity of boundary layers is almost constant at the level approximately 38 m.K/W indicating that before this test was initiated, oxygen and nitrogen filled these layers close to the highest possible level. Even though these boundary layers appear saturated with air, they provide a resistance to the passage of gas to and from the material core and thereby slow the overall aging process.

Polyisocyanurate product B

Figure 4 shows also large differences in thermal performance of skin and core layers. Contrary to the results obtained on PIR product A the skin layers show much better initial thermal performance than the core layers. Moreover, neither core nor skin layers appear to provide conclusive evidence at what thermal resistivity and time is the material saturated with air.

Lack of an apparent division between the primary and secondary stages of the aging process, see Figure 4, prevents application of the scaling factors. Since the scaling factors comprise the ratio of effective diffusivity coefficients (which is different for each stage of aging), the scaling factors may not be correctly applied without the determination of the division between two stages of the aging process.

A difference in thermal resistivity of skin and core layers was observed for this product. What are the causes of this difference? A difference in thermal resistance of the specimens made of the same polymer and having similar density may be attributed to one of the two factors: (1) a difference in the blowing agent concentration, (2) a difference in the extinction coefficient for radiation. The latter is proportional to the geometrical characteristic of the cell structure, distance between struts in particular.

To gain information on the blowing agent concentration, the measurements of thermal resistivity as a function of temperature were performed, see Figure 5. It may be observed that the blowing agent begins to condense at 275 K in the skin layers and at 273 K in the core layers. During these measurements the cold surface of the specimen being 5 K lower than the mean specimen temperature, see Bomberg et al [8], the blowing agent begins to condense at 270 and 268 K, implying that CFC 11 pressure is approximately 0.37 and 0.35 atmosphere for skin and core layers respectively. Thus, it appears that a higher CFC 11 pressure may explain only part of the improved thermal performance of the skin layers.

Polyisocyanurate product C

The aging curves of core specimens cut from product C are shown in Figures 6 and 7, each showing four specimens cut from one board, and in Figure 12 which shows six specimens cut from two different boards. In the latter case, three adjacent layers were cut from one board to characterize its cross-sectional variability.

To compare scatter of the experimental results, aging curves with the lowest and highest long-term thermal resistivity are selected from each of the Figures 6, 7 and 12 and presented in Figure 15. The bulk of the foam shows a high degree of uniformity. The aging curves that start from higher initial values, with time, come closer to those started at low initial thermal resistivity values. From the group of curves in Figure 15, as in research on sprayed polyurethanes [1,2], the curve with lowest long-term thermal resistivity was chosen as the reference curve for the product C.

Figures (8-11, 13 and 14) analyze the effect of gas barrier (facing layer). Observe that inclusion of aluminum foil in the gas barrier affected specimen weight and hence density was not calculated for faced specimens of product C. The aging curves with the lowest and highest long-term thermal resistivity were selected from each of the Figures 9, 10 and 11 and presented in Figure 16 together with the reference aging curve for the unfaced material cores. As seen in

Figure 16, presence of the facers introduces a significant retardation of the aging process, however, to a varying degree.

Figures 6-14, except for Figure 8, show smooth curves of thermal resistivity as a function of time. Figure 8 shows an experimental anomaly, namely an increase in measured thermal resistivity on 11th day. Since this anomaly was attributed to the specimen warpage, an additional weight was placed on the plates of the HFM apparatus (60th day), and the later readings of thermal resistivity appear to agree with those shown in Figures 9 and 10.

Figures 13 and 14 compare the effect of the surface area on the decay in thermal resistivity caused by diffusion through the specimen perimeter. The currently available data are insufficient to warrent a definite conclusion. However, the research is in progress and will be reported at at a later stage.

CONCLUDING REMARKS

This report examined application of slicing and scaling to boardstock products. Evaluating thermal performance of boardstock products introduced new considerations for the preparation of surface layers. For instance, when the product comprises a skin or a gas barrier that reduces the rate of gas diffusion through its surface, one must test only the diffusion through this surface. Comparing these tests with those performed without skins or facers one may evaluate the efficiency of skins and gas barriers in retarding the aging process.

New techniques for partial encapsulation of specimens were developed and with the help of these techniques both faced or skin layers were tested. The reference aging curves were then established for both core and surface specimens.

There appears, however, to be little ground for direct application of the scaling factors to non-uniform boardstock products [7]. Since a ratio of diffusion coefficients is needed to calculate the scaling factor, one must be able to measure the effective diffusion coefficients and divide the aging process into two stages. In the first stage, primary stage of aging process, the ratio of nitrogen diffusion coefficients should be used; in the secondary stage, the ratio of blowing agent diffusion coefficients is to be used. Since separating primary and secondary stages of aging was difficult for both non-uniform products A and B, the uncertainty in establishing scaling factors for non-homogenous boardstock products appear substantial.

While scaling factors could still be used for approximative estimate on non-uniformed foams, they cannot be used for any product provided with gas barriers. It has been shown during the examination of PIR product C that the efficiency of gas barrier vary from place to place. Because of this variability one must use computational procedures capable of addressing statistical variations in the retardation effect of facers.

While the scaling factors may not be directly applicable to skinned and faced boardstock products, the partial encapsulation technique developed in this work may find other applications. It was observed that establishing time dependence of thermal resistivity for partly encapsulated surface layers may help in evaluating variations in the manufacturing process. The use of partially encapsulated thin layers for predictive quality assessment should be further examined.

Acknowledgements

We express gratitude to Jim Walter Research Corporation and Demilec Chemicals Inc. for manufacturing and supplying the generic PIR products examined in this project.

References

1. Bomberg M.T., Kumaran M.K. 1989. Report on sprayed polyurethane foam with alternative blowing agents. CFCs and the Polyurethane Industry: Volume 2, p. 112 -128.

2. Kumaran M.K.., Bomberg M.T. 1990. Thermal performance of sprayed polyurethane foam insulation with alternative blowing agents. J Thermal Insulation, Vol. 14, July 1990, p. 43-58.

3. Edgecombe F.H., Progress in evaluating long-term thermal resistance of cellular plastics, J. Thermal Insulation, Vol 13, Oct 1989, p. 105-123.

4. Schwartz N.V., Bomberg M.T., Kumaran M.K. 1989. Measurement of the rate of gas diffusion in rigid cellular plastics. J Thermal Insulation, Vol.13, 1989, p. 48-61.

5. Kumaran M.K., Bomberg M.T., Marchand R.G., Creazzo J.A., Ascough M.R. 1989. A Method for evaluating the effect of blowing agent condensation on sprayed polyurethane foams. J. Thermal Insulation, Vol.13, Oct. 1989, p. 123-137.

6. Bomberg M., and K.R.Solvason, "Comments on calibration and design of a heat flow meter", ASTM, STP 789, 1983, p. 272-292.

7. Bomberg M.T., "Scaling factors in aging of gas-filled cellular plastics", J Thermal Insulation Vol.13, January 1990, p. 149-159.

8. Bomberg M.T., Kumaran M.K., Ascough M.R., Sylvester R.G., "Effect of Time and Temperature on R-value of Rigid Polyurethane Foams", Polyurethane 90 SPI Conference, Orlando, Fla, 1-3 October 1990, p. 420-431

Table 1. Description of test specimens prepared from polyisocyanurate product C.

Testing purpose *& size	Specimen description and properties: code number	thickness mm	density kg/m^3	encapsulation type	initial r-value m^2K/W	Figure number
series 1						
Control 30 cm	2NE	26.89	-	2 facers	53.3	
	2NW	25.87	-	2 facers	53.8	
	2SE	26.59	-	2 facers	56.0	
	2SW	25.29	-	2 facers	54.9	
core 30 cm	3NE	5.01	28.1	none	49.4	Fig 6
	3NW	5.00	27.9	none	49.4	
	3SE	5.00	28.0	none	49.9	
	3SW	4.99	27.9	none	50.0	
core 30 cm	9NE	5.44	27.7	none	49.8	Fig 7
	9NW	5.27	27.6	none	49.2	
	9SE	5.21	27.3	none	49.5	
	9SW	5.27	27.5	none	49.8	
top 30 cm	4NE	7.30	-	(b)	51.4	Fig 8
	4NW	7.16	-	(b)	50.9	
	4SE	7.10	-	(b)	51.6	
	4SW	7.25	-	(b)	51.9	
top 30 cm	10NE	5.35	-	(b)	53.2	Fig 9
	10NW	5.40	-	(b)	53.6	
	10SE	4.96	-	(b)	50.6	
	10SW	5.21	-	(b)	52.5	
bottom 30 cm	5NE	7.35	-	(b)	50.9	Fig 10
	5NW	7.28	-	(b)	52.7	
	5SE	7.40	-	(b)	51.9	
	5SW	7.37	-	(b)	51.6	
bottom 30 cm	11NE	5.46	-	(b)	52.6	Fig 11
	11NW	5.26	-	(b)	51.2	
	11SE	5.24	-	(b)	52.8	
	11SW	5.17	-	(b)	52.9	

Testing purpose & size	code number	thickness mm	density kg/m^3	encapsulation type	initial r-value m^2K/W	Figure number
		Specimen description and properties				
series 2						
control	27	27.8	-	2 facers	54.0	
30 cm	34	26.5	-	2 facers	54.3	
control	12	25.2	-	2 facers	54.6	
60 cm	37	26.3	-	2 facers	55.6	
layers	30NE	5.44	30.4	none	52.4	Fig 12
30 cm	30NW	5.43	29.5	none	51.9	
	30SE	5.46	29.5	none	52.2	
	33NE	5.34	29.9	none	52.4	
	33NW	5.43	28.9	none	51.9	
	33SE	5.53	29.8	none	52.2	
top	31NE	11.22	-	(b)	55.4	Fig 13
bottom	31NW	10.92	-	(b)	54.6	
30 cm	31SE	10.65	-	(b)	55.5	
	31SW	10.59	-	(b)	54.8	
top	15NE	11.30	-	(b)	52.5	Fig 14
bottom	18WW	10.90	-	(b)	56.3	
60 cm	40SE	11.23	-	(b)	53.1	
	43SW	11.06	-	(b)	56.5	

Figure captions.

Figure 1. Distribution of density in the PIR product A.

Figure 2. Schematic of partial encapsulation for surface layers:
(a) material with skins
(b) material with gas barriers

Figure 3. Aging curves for skin and core layers of PIR product A.

Figure 4. Aging curves for boundary and core layers of PIR product B.

Figure 5. Temperature dependence of thermal resistivity of PIR product B.

Figure 6. Aging curves for core layers of PIR product C.

Figure 7. Aging curves for core layers of PIR product C.

Figure 8. Aging curves for layers cut from surface 1 of the PIR product C.

Figure 9. Aging curves for layers cut from surface 1 of the PIR product C.

Figure 10. Aging curves for layers cut from surface 2 of the PIR product C.

Figure 11. Aging curves for layers cut from surface 2 of the PIR product C.

Figure 12. Aging curves for core layers of PIR product C.

Figure 13. Aging curves for surface layers of PIR product C.

Figure 14. Aging curves for surface layers of PIR product C, specimens 60 x 60 cm.

Figure 15. Aging curves for core layers of PIR product C.

Figure 16. Comparison of extreme aging curves for different layers of PIR product C.

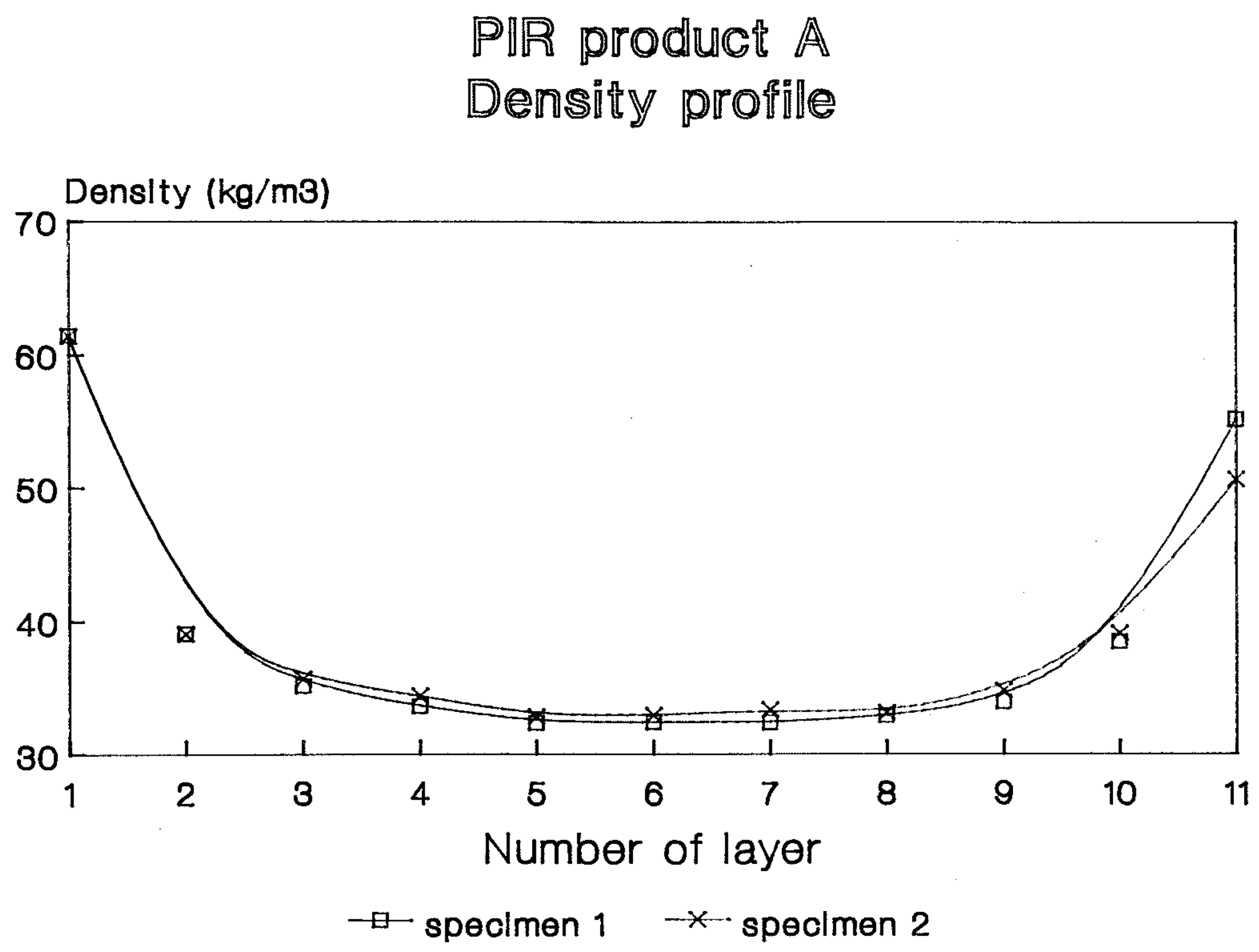
PIR product A
Density profile
Density (kg/m3)
70
60
50
40
30
1
2
3
4
5
6
7
8
9
10
11
Number of layer
specimen 1
specimen 2

Figure 1

Partial encapsulation for products with (a) skins, (b) gas barriers

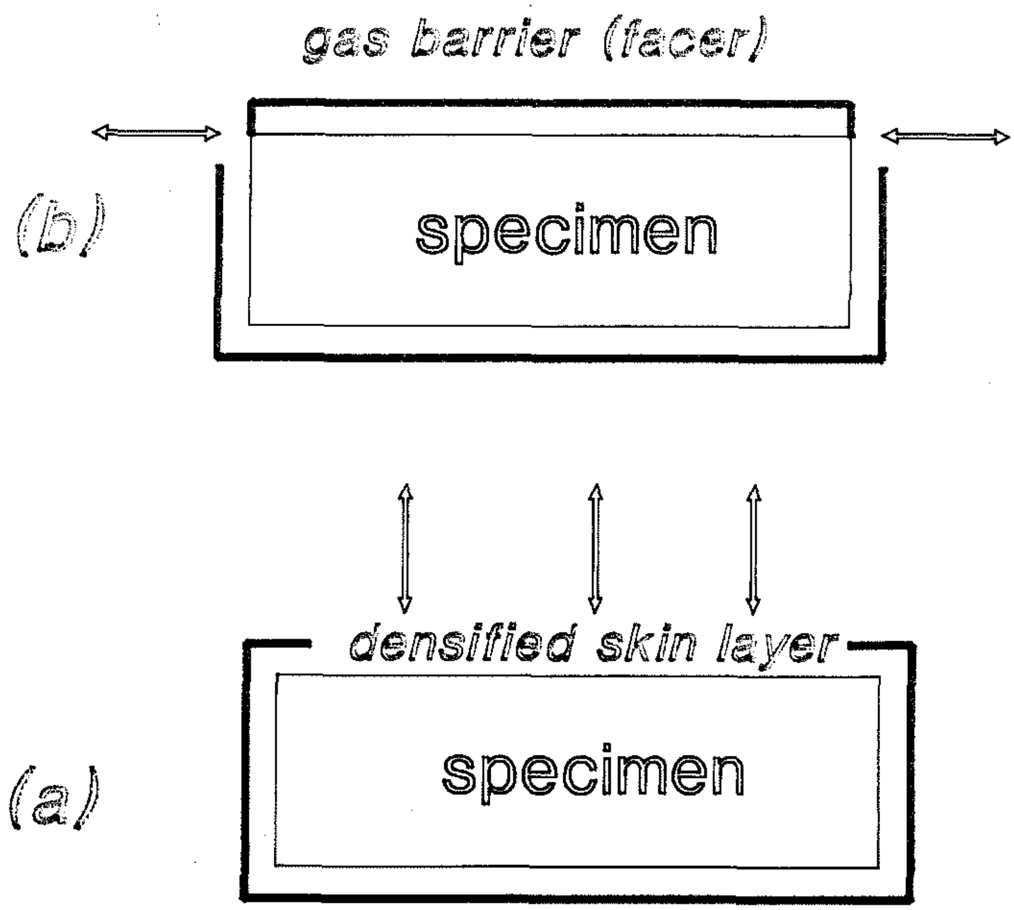

Note : The arrows indicate path of gas flow

Figure 2

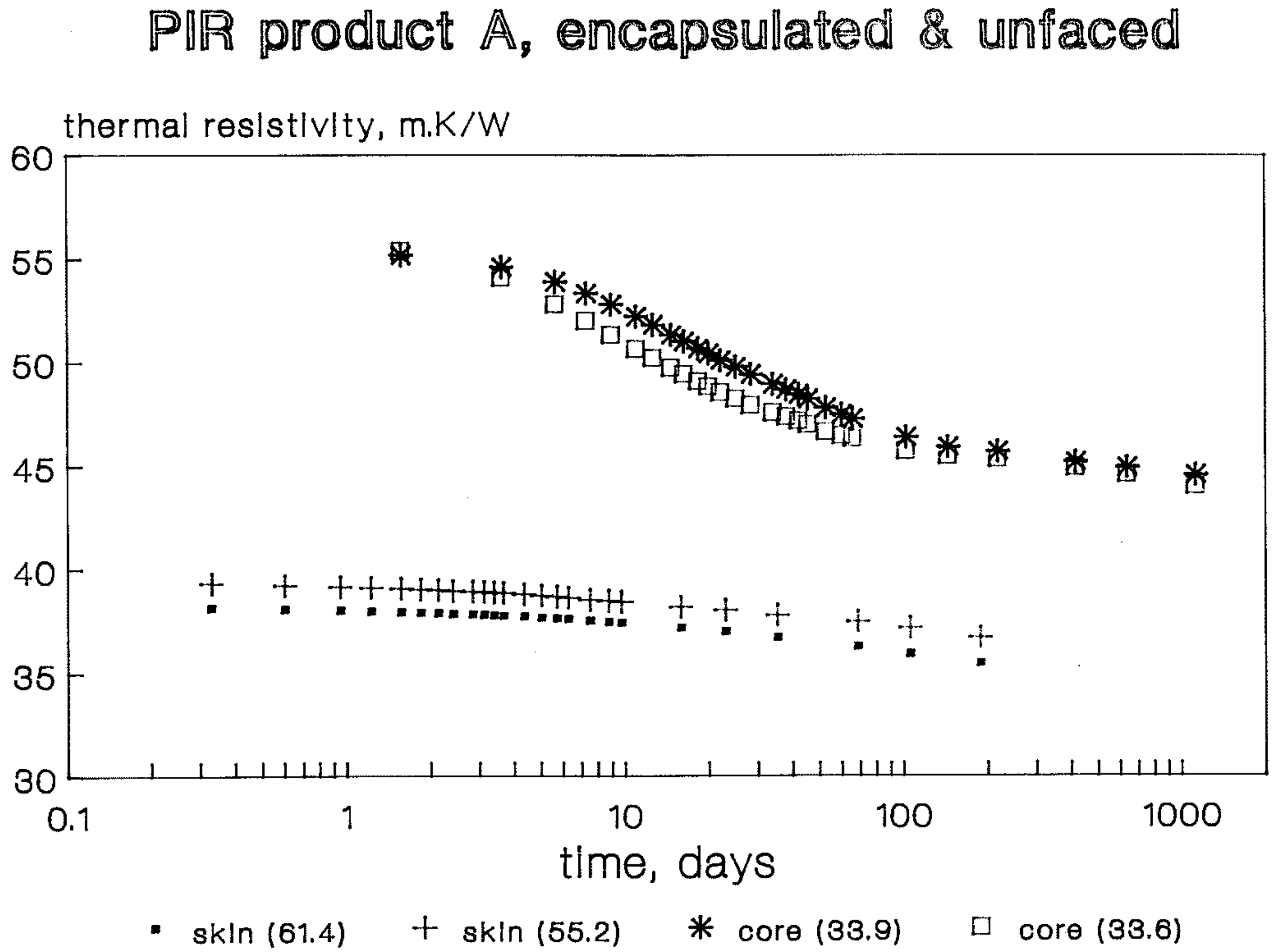
PIR product A, encapsulated & unfaced
thermal resistivity, m.K/W
60
55
50
45
40
35
30
0.1
1
10
100
1000
time, days
skin (61.4)
skin (55.2)
core (33.9)
core (33.6)

Figure 3

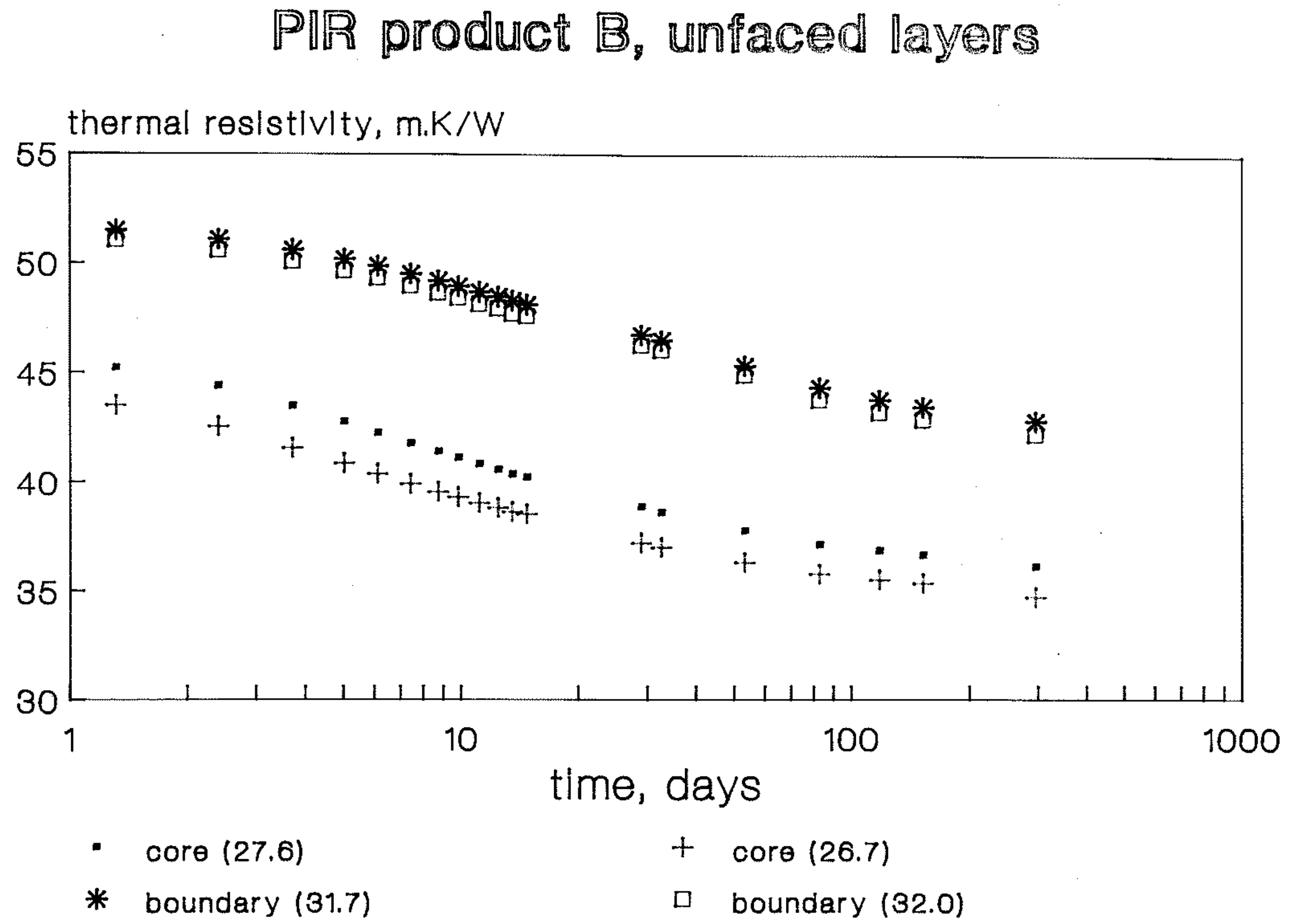

PIR product B, unfaced layers
thermal resistivity, m.K/W
55
50
45
40
35
30
1
10
100
1000
time, days
core (27.6)
core (26.7)
boundary (31.7)
boundary (32.0)

Figure 4

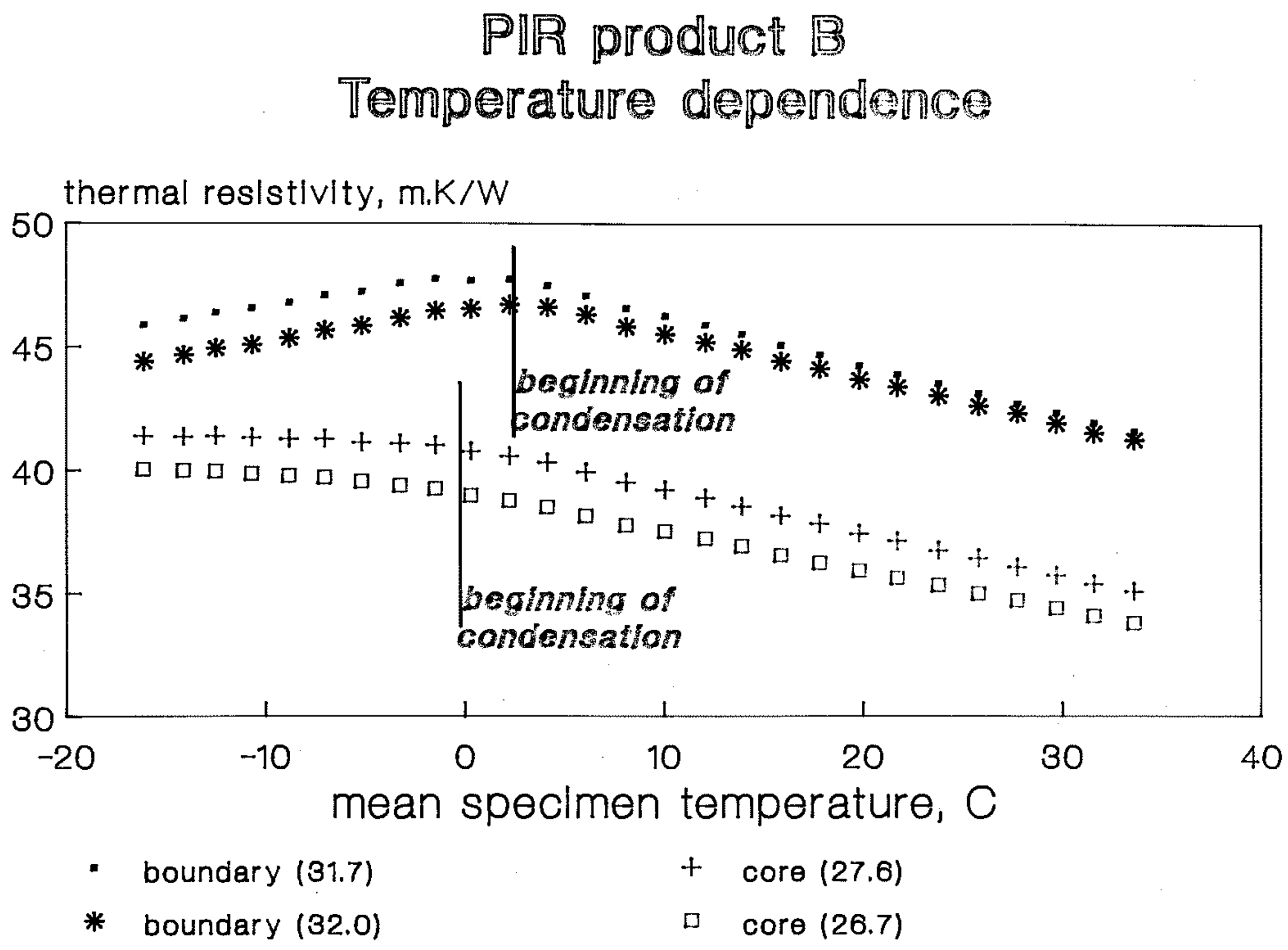
PIR product B
Temperature dependence
thermal resistivity, m.K/W
50
45
40
35
30
-20
-10
0
10
20
30
40
mean specimen temperature, C
beginning of condensation
beginning of condensation
boundary (31.7)
boundary (32.0)
core (27.6)
core (26.7)

Figure 5

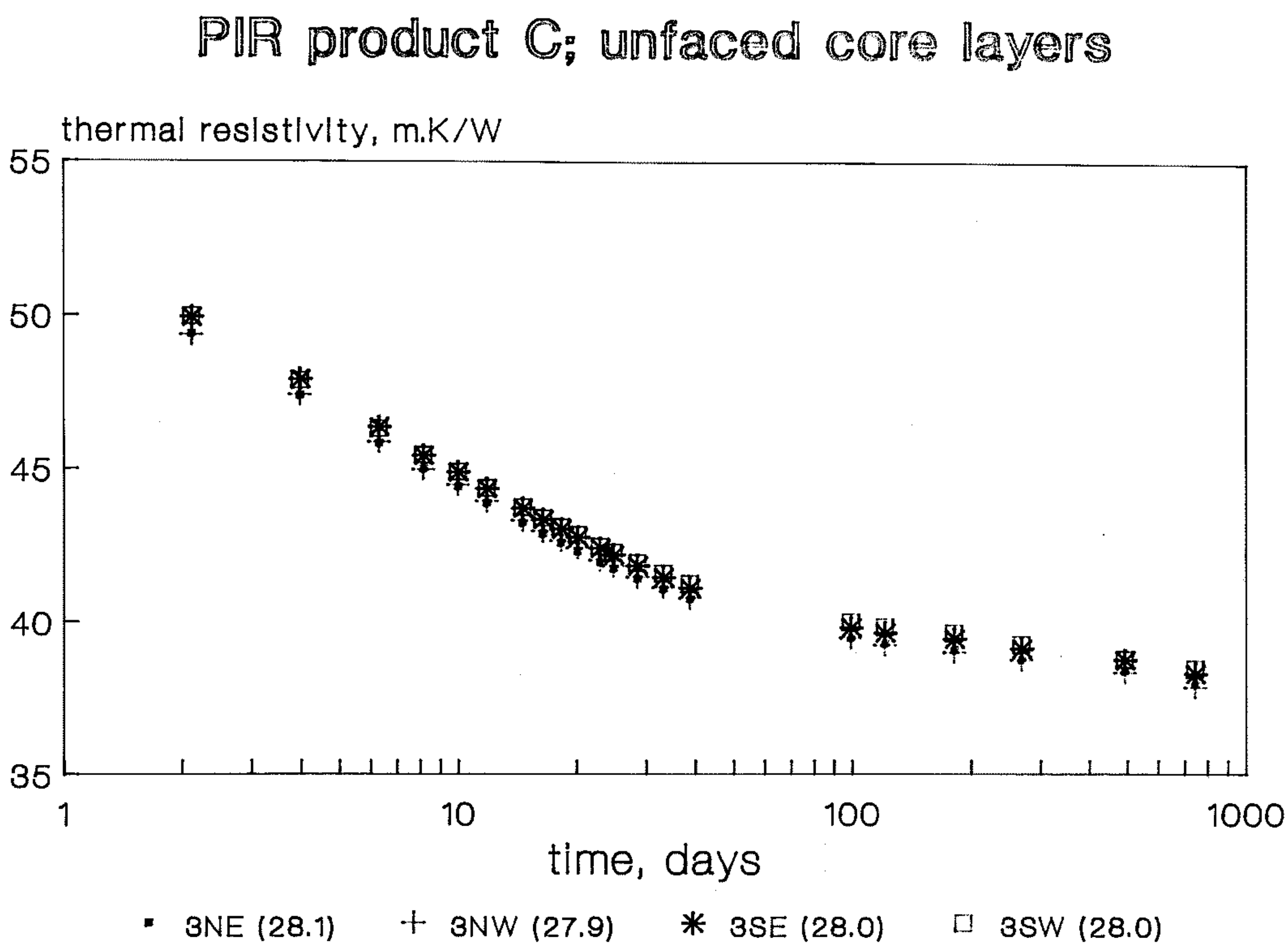
PIR product C; unfaced core layers
thermal resistivity, m.K/W
55
50
45
40
35
1
10
100
1000
time, days
3NE (28.1)
3NW (27.9)
3SE (28.0)
3SW (28.0)

Figure 6

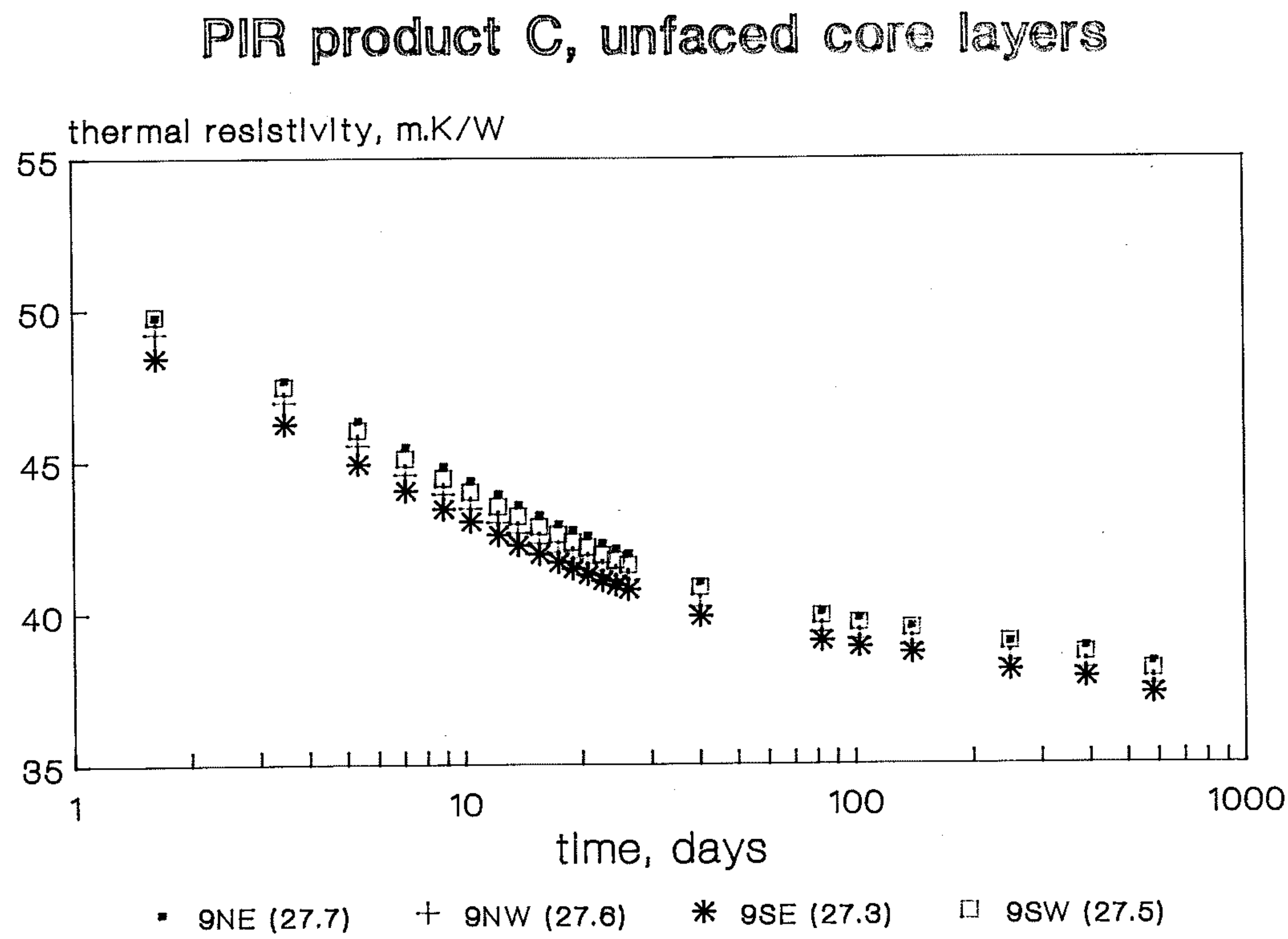
PIR product C, unfaced core layers
thermal resistivity, m.K/W
55
50
45
40
35
1
10
100
1000
time, days
9NE (27.7)
9NW (27.6)
9SE (27.3)
9SW (27.5)

Figure 7

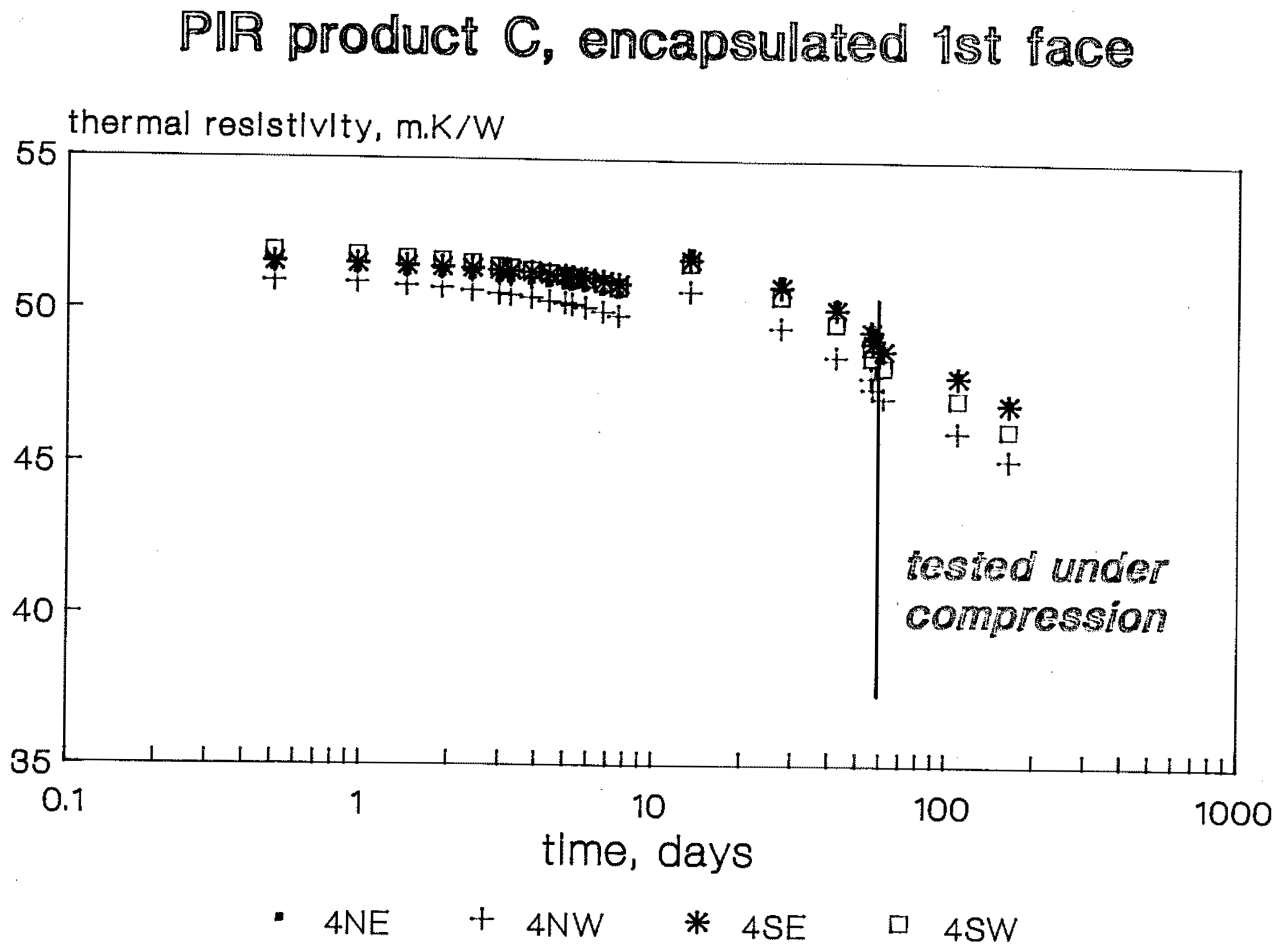
PIR product C, encapsulated 1st face
thermal resistivity, m.K/W
55
50
45
40
35
0.1
1
10
100
1000
time, days
tested under compression
4NE
4NW
4SE
4SW

Figure 8

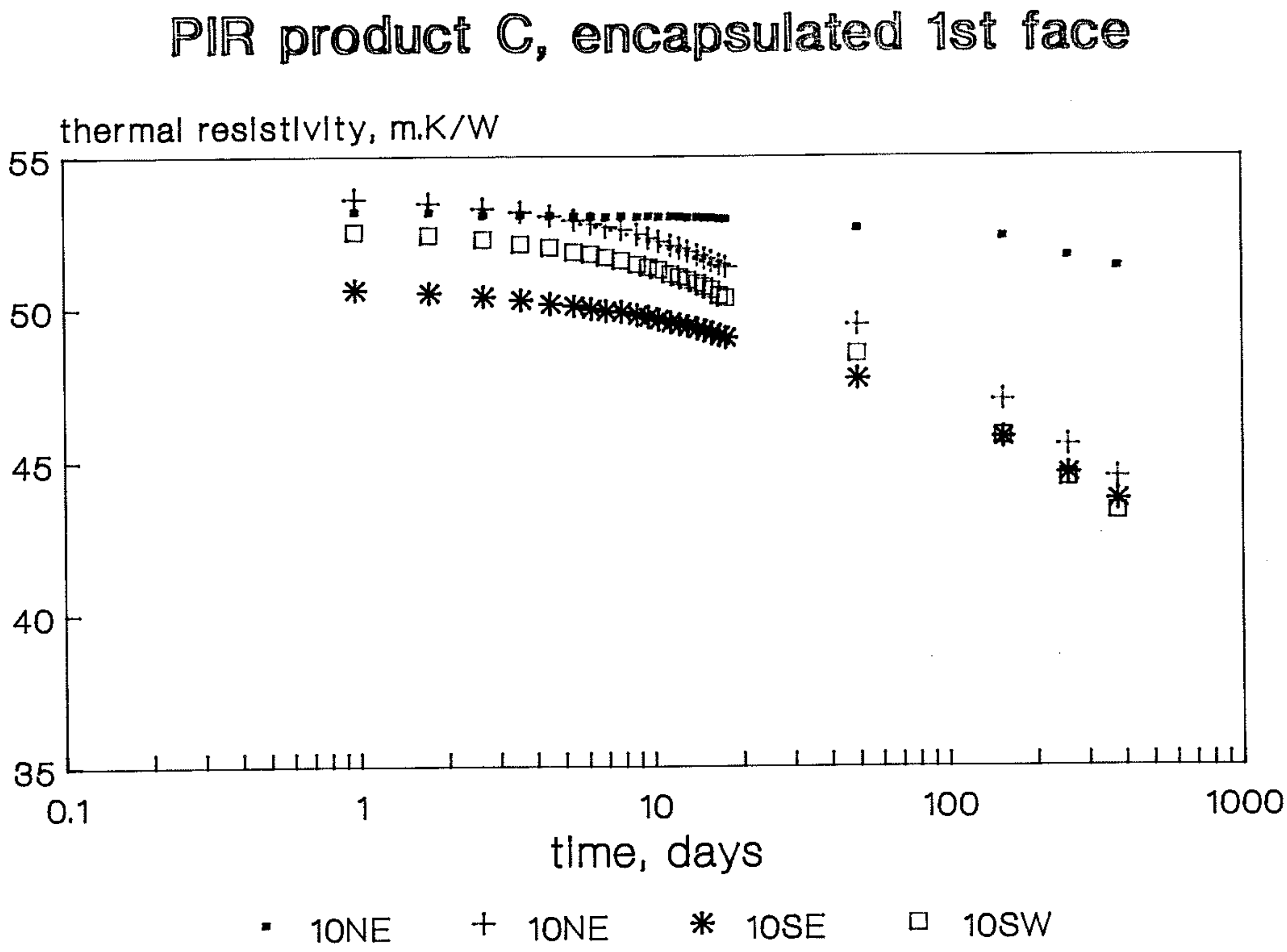
PIR product C, encapsulated 1st face
thermal resistivity, m.K/W
55
50
45
40
35
0.1
1
10
100
1000
time, days
10NE
10NE
10SE
10SW

Figure 9

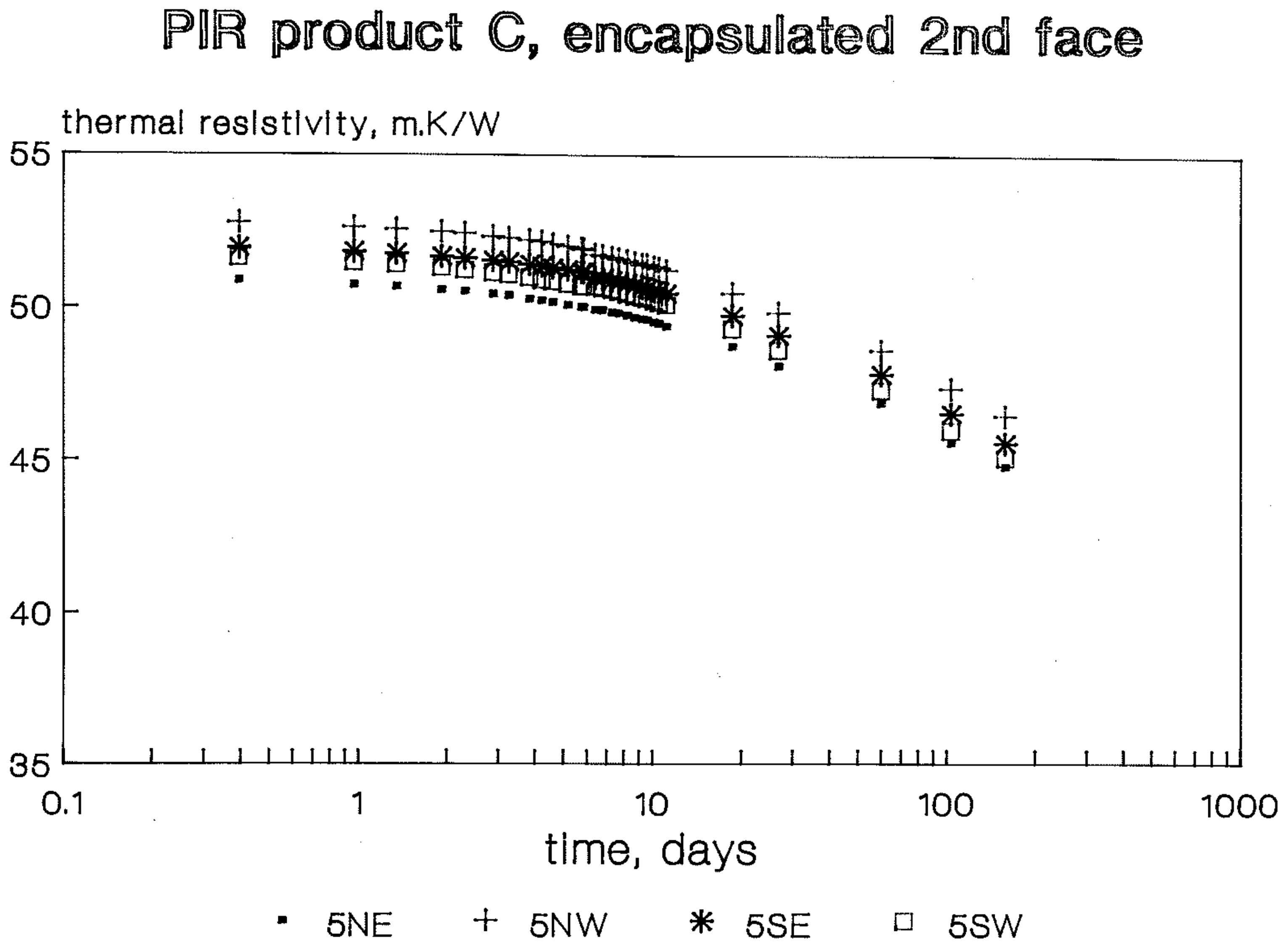
PIR product C, encapsulated 2nd face
thermal resistivity, m.K/W
55
50
45
40
35
0.1
1
10
100
1000
time, days
5NE
5NW
5SE
5SW

Figure 10

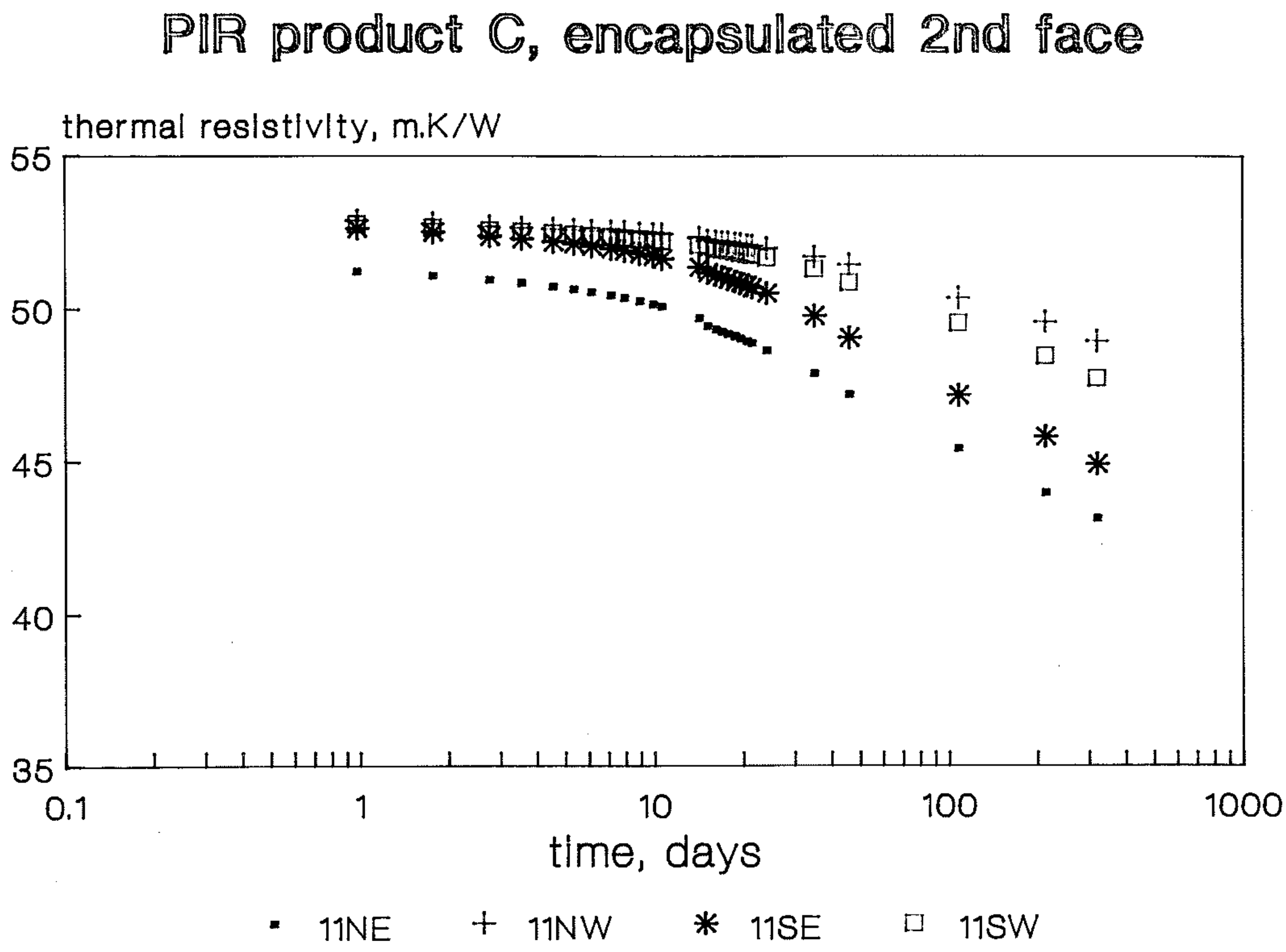
PIR product C, encapsulated 2nd face
thermal resistivity, m.K/W
55
50
45
40
35
0.1
1
10
100
1000
time, days
11NE
11NW
11SE
11SW

Figure 11

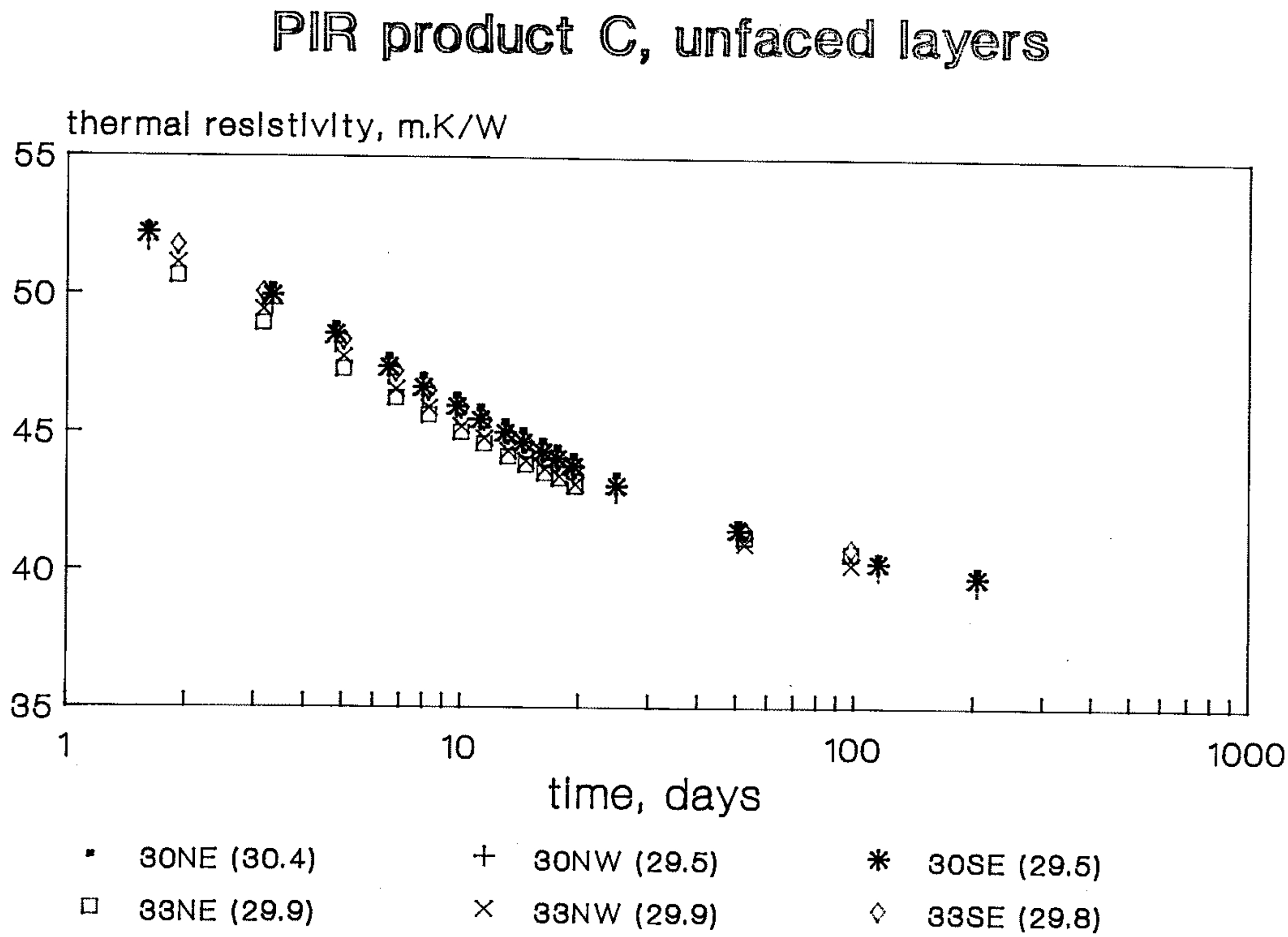
PIR product C, unfaced layers
thermal resistivity, m.K/W
55
50
45
40
35
1
10
100
1000
time, days
30NE (30.4)
30NW (29.5)
30SE (29.5)
33NE (29.9)
33NW (29.9)
33SE (29.8)

Figure 12

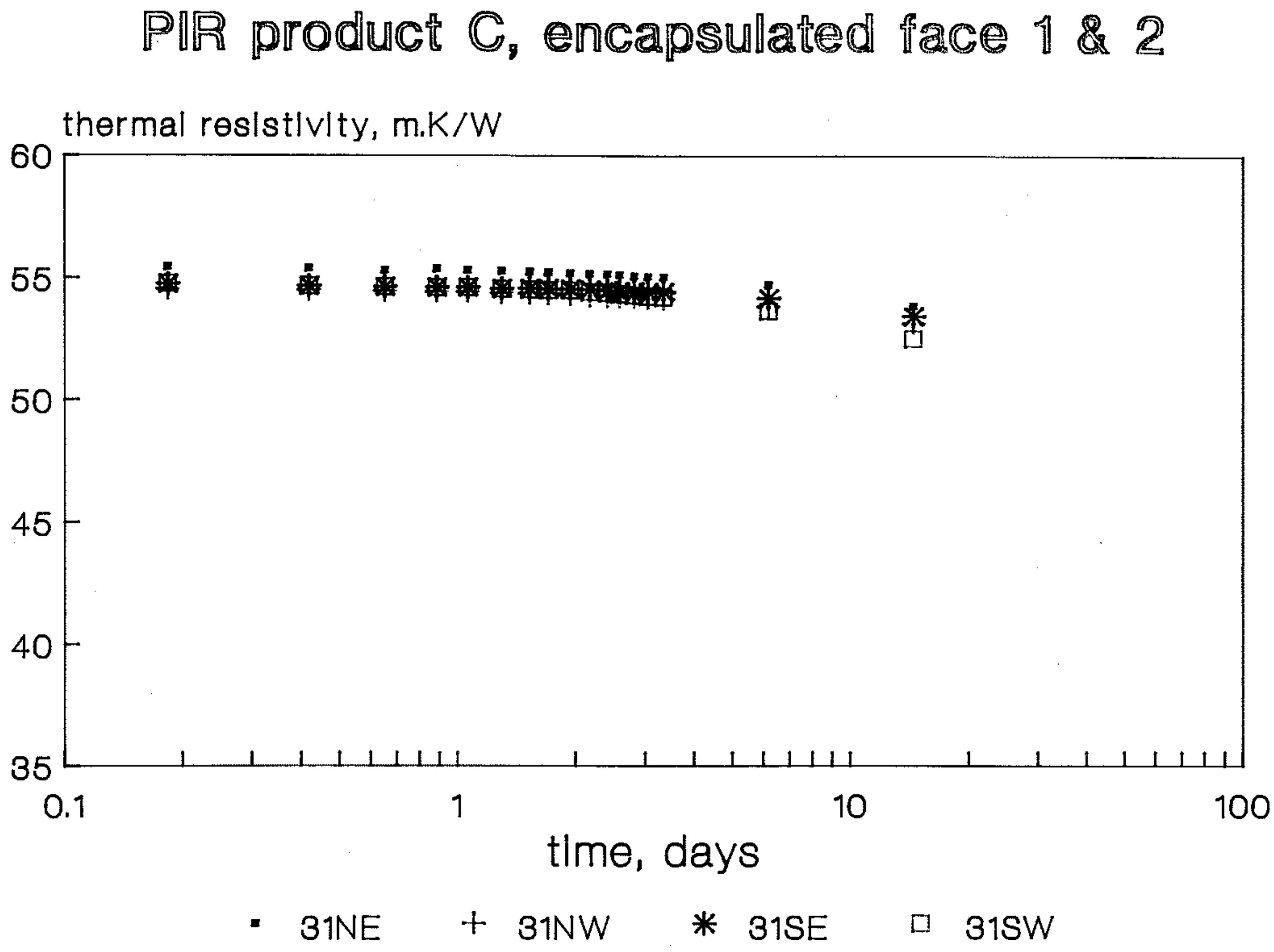
PIR product C, encapsulated face 1 & 2
thermal resistivity, m.K/W
60
55
50
45
40
35
0.1
1
10
100
time, days
31NE
31NW
31SE
31SW

Figure 13

PIR product C, encapsulated face 1 & 2
Specimens 60 x 60 cm

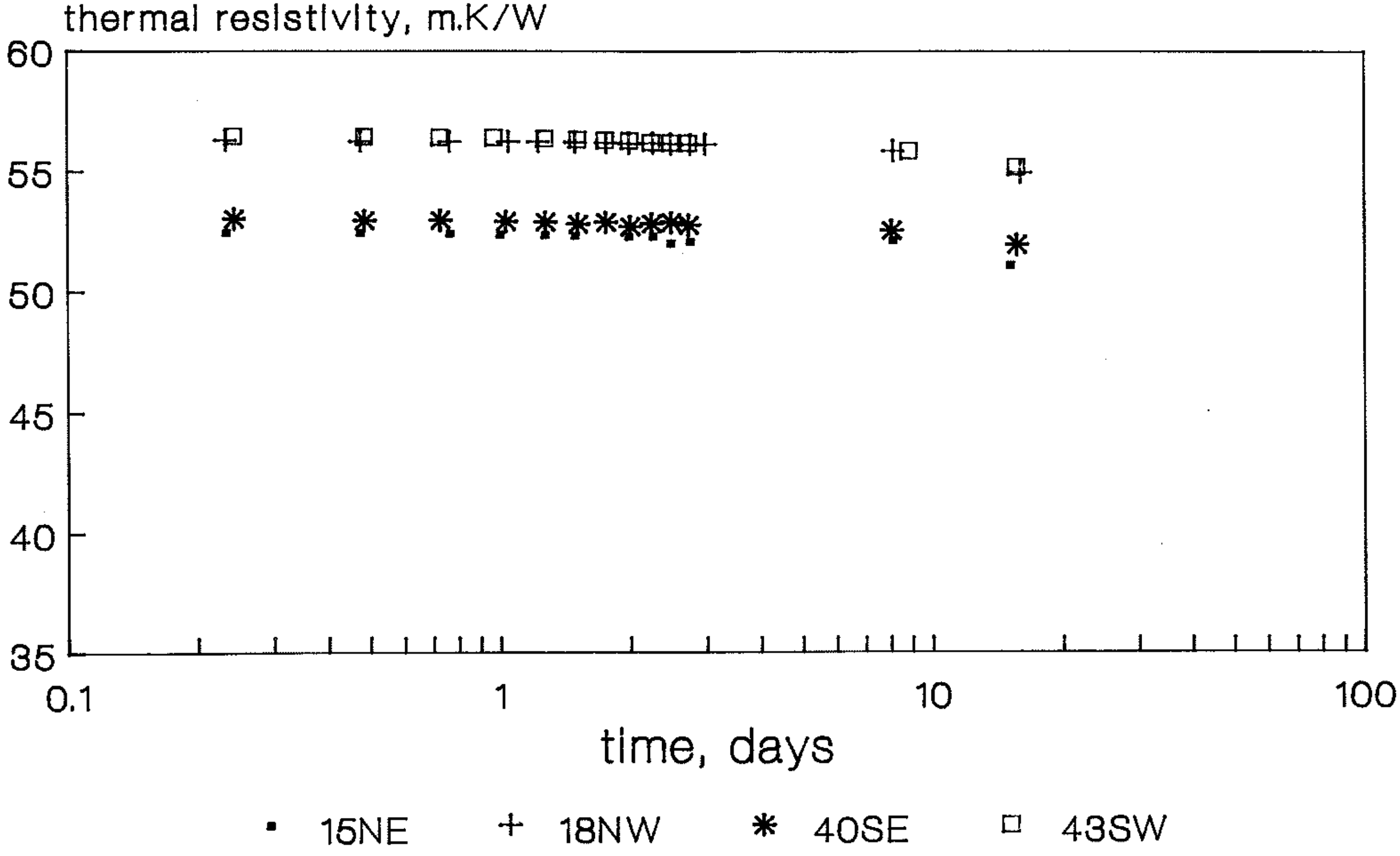

Figure 14

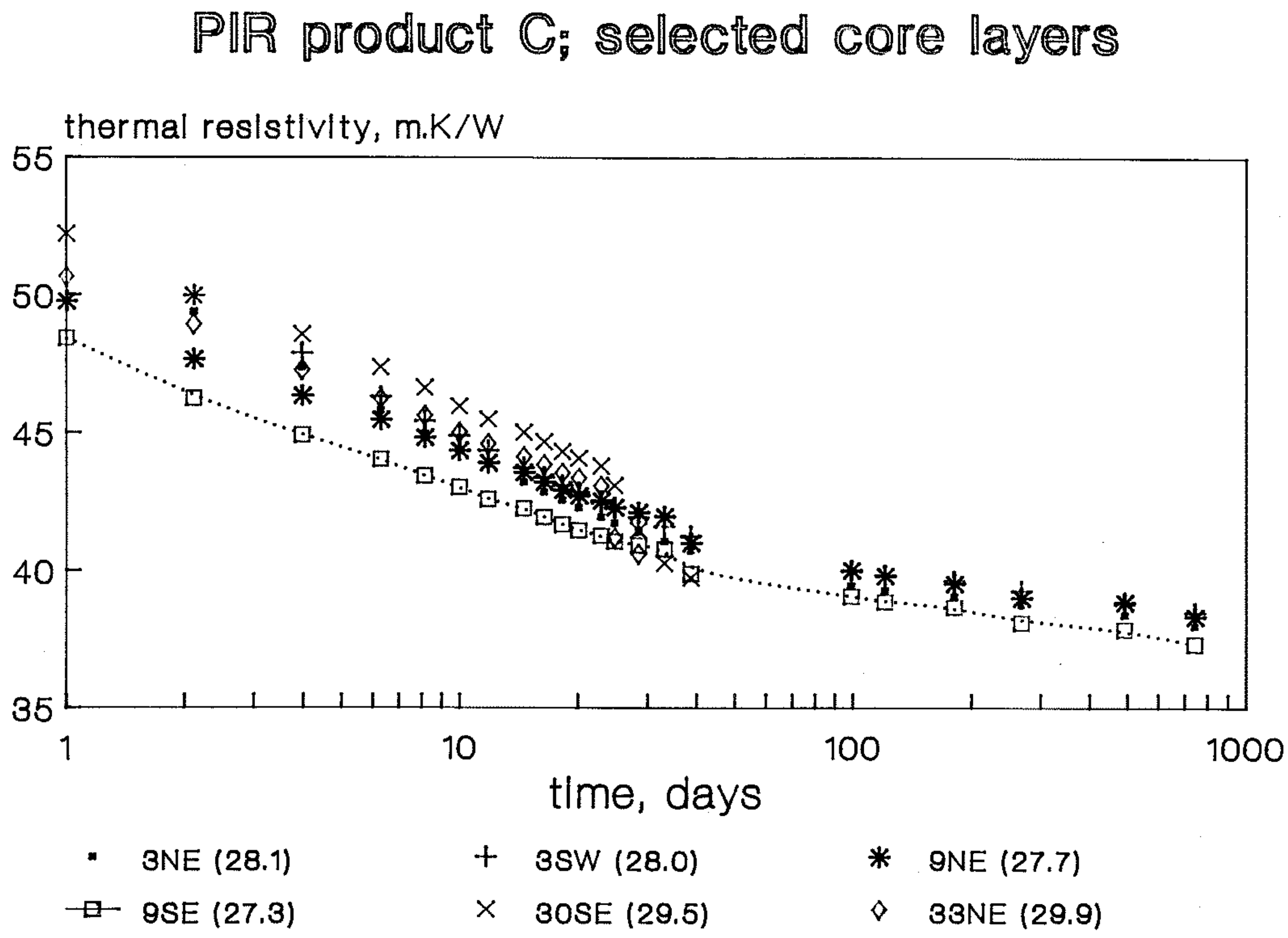
PIR product C; selected core layers
thermal resistivity, m.K/W
55
50
45
40
35
1
10
100
1000
time, days
3NE (28.1)
3SW (28.0)
9NE (27.7)
9SE (27.3)
30SE (29.5)
33NE (29.9)

Figure 15

PIR product C; core, faces and boards

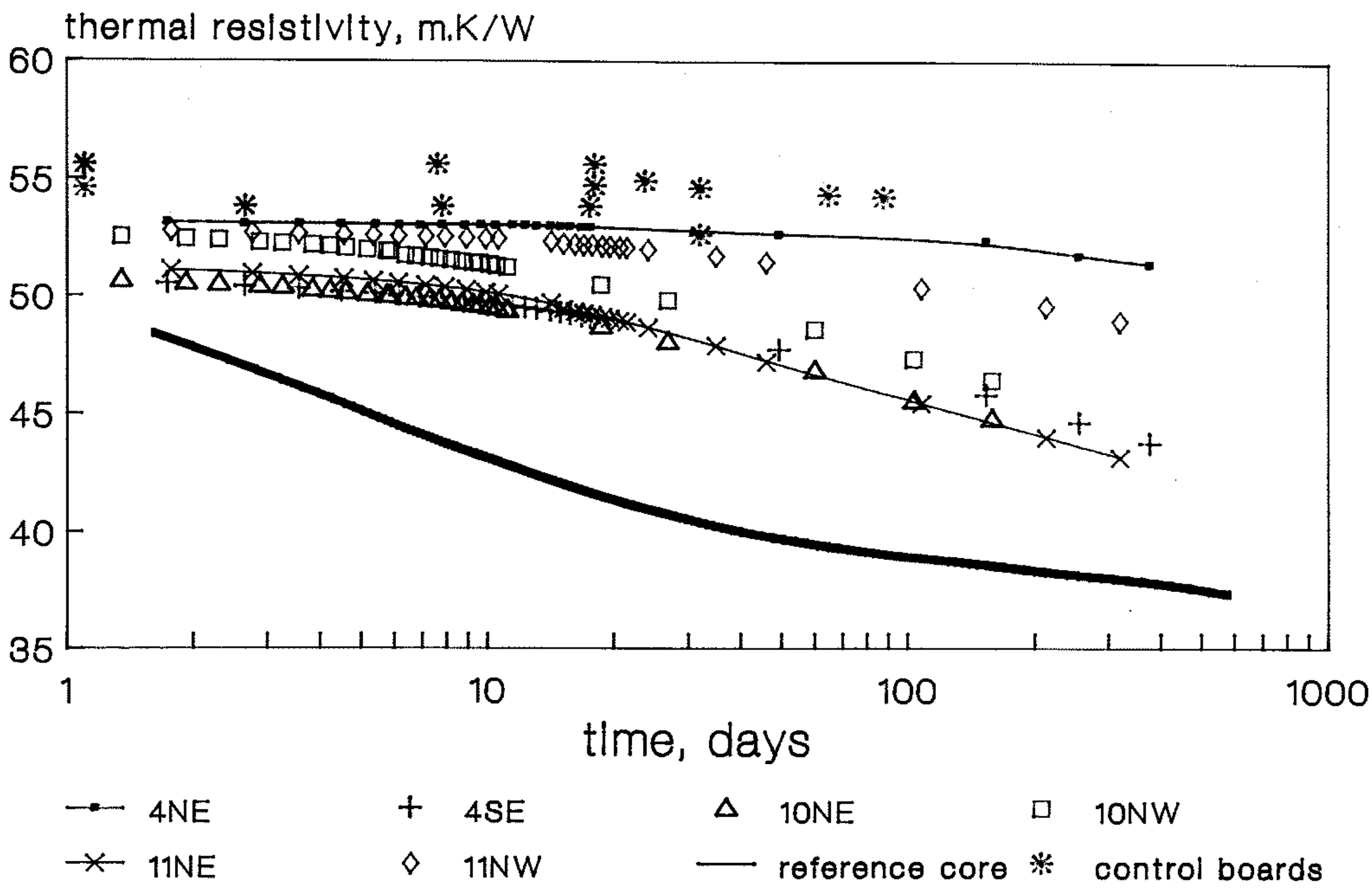

Figure 16